ZESZYTY NAUKOWE POLITECHNIKI ŚLĄSKIEJ 1995
Seria: ENERGETYKA z. 126 Nr kol. 1281

Andrzej WITKOWSKI, Michał STROZIK
Instytut Maszyn i Urządzeń Energetycznych
Marek MIRSKI
Raciborska Fabryka Kotłów „RAFAKO"

TURBULENCE AND UNSTEADINESS MEASUREMENTS DOWNSTREAM OF A ROTOR BLADE ROW OF AN AXIAL LOW PRESSURE COMPRESSOR STAGE

Summary. A full digital operating measuring technique based on triple split fiber probe, straight and 90° was built up, in order to determine the unsteady flow field downstream of the rotor of axial flow compressor stage, in stationary frame of reference. Anemometer outputs at points relative to impeller blades channel are sampled periodically with reference to pulses from optical incremental shaft encoders connected directly with the shaft of the impeller. The objective to the experimental programme was to investigate the wake flow at chosen diffrent axial locations downstream of the rotor and on the centerline of the stator passage. At chosen axial position 39 radial measurements was carried out in order to get the span–wise characteristics of the unsteady flow. The secondary flow field downstream of the rotor blade is discussed.

BADANIE TURBULENCJI ORAZ ZJAWISK NIEUSTALONYCH NA WYLOCIE Z WIEŃCA ŁOPATKOWEGO KOŁA WIRNIKOWEGO OSIOWEGO NISKOCIŚNIENIOWEGO STOPNIA SPRĘŻAJĄCEGO

Streszczenie. Opracowano centralnie sterowany system pomiarowy nieustalonego pola przepływu za kołem wirnikowym osiowego stopnia sprężającego w układzie bezwzględnym. Sygnały anemometryczne próbkowane są periodycznie pod wpływem impulsów generowanych poprzez przetwornik optoelektryczny sprzężony bezpośrednio z wałem wirnika. Celem badań było rozpoznanie charakterystyk śladów pozałopatkowych w wybranych przekrojach kontrolnych za kołem wirnikowym oraz wzdłuż linii środkowej kanału międzyłopatkowego statora. W wybranym przekroju osiowym przeprowadzono sondowanie przepływu na 39 promieniach w celu określenia rozkładu nieustalonego pola prędkości wzdłuż wysokości kanału. Przeanalizowano pole przepływów wtórnych w przekroju wylotowym łopatek koła wirnikowego.

UNTERSUCHUNGEN DER TURBULENZ UND NICHSTTIONÄREN VORGÄNGE AM AUSTRITT EINES SCHAUFELKRANZES DES ROTORS VON AXIALEN NIEDRDRUCK VERDICHTERSTUFE

Zusammenfassung. Ein zentralgesteuertes Meßsystem für die Messung von nichstationären Strömingfledes nach dem Rotor einer axialen verdichterstufe im Absoluten Koordinatensystem wurde bearbeitet. Meßsignale vom Anemometer sind periodisch getastet unter dem Einfluß des erzeugenden Impulsen in Opto–elektrischem mit der Welle verbundenen Geber. Ziel der Untersuchungen war die Ermittlung von Spurenkennlinien nach Schaufeln in ausgewählten Kontrolschnitten und im Raum hinter dem Rotor und entlängs mittleren Linie des Zwischenschaufelkanals des Stators.

1. INTRODUCTION

An understanding of the flow physics associated with the leakage and secondary flows and with the wake boundary layer interaction in turbomachinery and the ability of the computer codes to predict its effects on the blade row performance are essential for eventual integration of the unsteady effects into the design process. Most of the present analysis and design methods in turbomachinery are based on steady aerodynamics. The unsteady flow associated with blade row interaction has a major influence on the flow field, boundary layers turbulence intensities, separation, vibration and noise. This requires more sophisticated design methods, including the possibility to calibrate numerical schemes and their turbulence modeling. There is a need to get a better understanding of the three dimensional unsteady flow in a blade row including the influence of rotor stator interactions.

The objective of the present study is to investigate the characteristic flow parameters which govern the unsteady flow field inside of a axial flow compressor blade row spacing and stator passage. Particularly:

1) upstream and downstream flow field of the rotor particularly in the rotor tip region,
2) transport of rotor wakes in the blade row spacing and stator passage,
3) the unsteady flow associated with rotor stator interaction.

All measurements have been carried out with triple split sensor and with five hole probes. So the mean average velocity obtained with both probe could be compared.

2. EXPERIMENTAL FACILITY

The measurements were carried out in the axial flow low pressure compressor stage described in detail in the others authors papers [1], [2]. It consists of the impeller of hub annulus wall diameter ratio 0.56 with diameter of the annulus wall being 1.0 m, discharge back stator vane and the outflow curvilinear diffuser with throttling blades.

The model compressor stage is set on the suction side on the measuring collector (fig. 1). The main elements of the research stand are a measuring pipeline with aerodynamically designed inlet nozzle for the measurement of flow intensity, a 30 kW direct current motor mounted in the cradle allowing for continous rotation changes up to 3000 r.p.m. In order to evaluate the overall performance characteristics of the rotor, conventional aerodynamic measurements were carried out in two probe measuring planes.

The dimensionless parameters of four points of impeller overall characteristics selected for further detailed flow investigation are also shown in table 1. In the present paper only the results of flow investigation at maximum value of flow coefficient has been discussed.

Table 1

Compressor impeller dimensionless parameters at design and off-design conditions

	Flow rate coefficient $\varphi = C_m/U_2$	Pressure coefficient $\psi = 2\Delta Pc/\rho U_2^2$	Inner impeller efficiency η_i
1	0,426	0,2871	0,922
2	0,405	0,3235	0,948
3	0,3701	0,3717	0,946
4	0,326	0,409	0,923

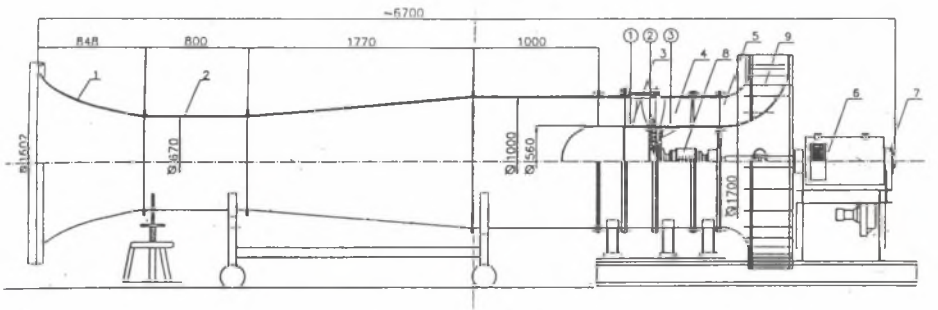

Fig. 1. Test stand

Rys. 1. Stanowisko badawcze

3. MEASUREMENT TECHNIQUE AND TEST PROGRAM

3.1. Unsteady Flow Field Measurements

The flow field downstream of the impeller and on centerline of the stator blade passage have been sampled periodically using a straight and 90° triple splite fiber probes (fig. 2). The axial and tangential velocity components lie in a plane which is perpendicular to the axis of the straight version of probes and are easily measured. The third velocity component should be measured by a separate 90° probe as shown in figure 2. That probes has very high spatial resolution and allows measurement without restrictions in the flow angle. The positions of this probes are always optimal with respect to every particular flow situation and they must not be revolved during measurements. It is possible to save the measuring time in a significant way. It should also be emphasised, that this probe is more robust and less sensitive to contamination than wire probe. The working principle of the triple split fiber probes is based on the variation of the local heat transfer on cylinders in a cross flow. A more detail description of the triple split fiber probes and their calibration procedure is given in the papers [3], [4].

The data from the triple split anemometer were acquired and recorded in digital form via three channel anemometer system, three parallel working sample hold amplifiers, analog multiplexer and 12 bit analog digital converter. An optical shaft encoder provided a puls for every 0.1° of impeller rotation realising A/D processing at the moment synchronised with the chosen angle positions of the impeller [4]. The IBM PC/AT 486DX computer intelligence to run the system, analyse data and provide control.

3.2. Test programe

The objective of the investigation reported in this paper was to determine:

- the decay wake of the flow at chosen different axial locations downstream of the rotor and on the centerline of the stator passage (fig. 3),
- the spanwise characteristics of the unsteady flow at chosen axial position,
- secondary flow field plots.

3.3. Data reduction

Ensemble averaging was the main data reduction method used in the experiments. It is particularly suited for the investigation of periodically unsteady flow process, which makes it possible to separate periodic fluctuations from random fluctuations [5], [6]:

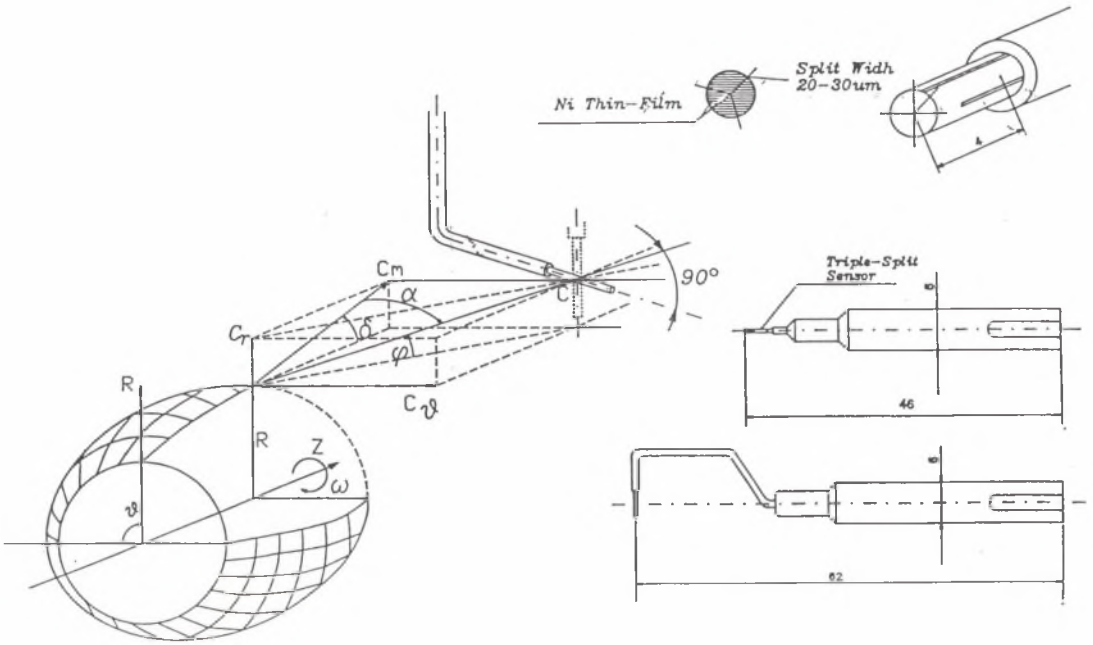

Fig. 2. Outline of Triple Split Probe

Rys. 2. Sonda termoanemometryczna z trójdzielną warstwą

the ensemble – averaged mean velocity

$$\vec{\bar{C}}_i = -\frac{1}{N}\sum_{n=1}^{N} C_{i,n} \tag{1}$$

the ensemble – averaged mean angle

$$\bar{\alpha}_i = \frac{1}{N}\sum_{n=1}^{N} \alpha_{i,n} \tag{2}$$

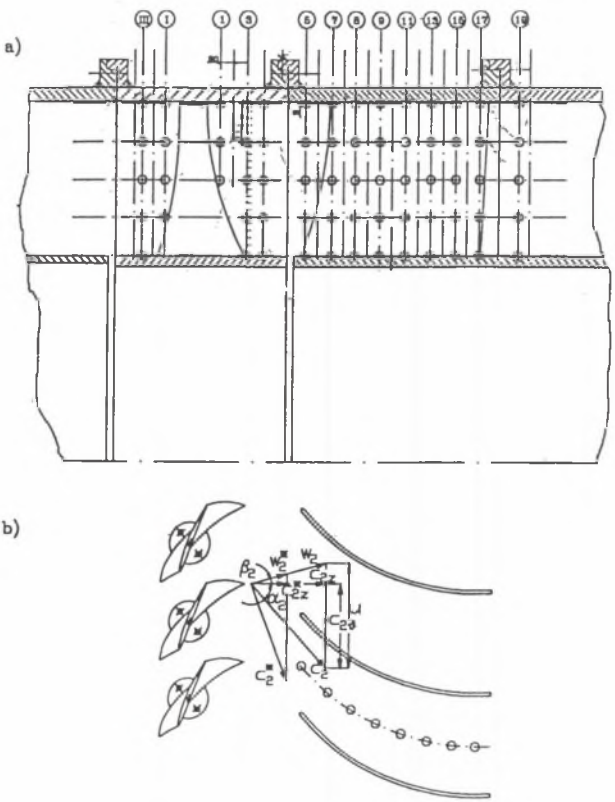

Fig. 3. Locations of Measurements

Rys. 3. Lokalizacja punktów pomiarowych

the mean velocity vector

$$\overline{\tilde{C}} = \frac{1}{N} \sum_{i=1}^{N} \sum_{n=1}^{N} C_{i,n} \tag{3}$$

where N denotes the number of revolutions and i the index for circumferential direction.

Now we can determine the absolute and relative components of velocity in accordance with fig. 3:

$$\tilde{C}_{zi} = \tilde{C}_i \cos \alpha_i \tag{4}$$

in circumferential direction

$$\tilde{C}_{\vartheta i} = \tilde{C}_i \sin \tilde{\alpha}_i \tag{5}$$

in radial direction

$$\tilde{C}_{ri} = \tilde{C}_i \sin \tilde{\varphi}_i \tag{6}$$

the velocity in the relative frame obtained from the absolute values and a vector addition of the circumferential speed

$$\tilde{W}_{i,n} = \sqrt{\tilde{C}_{zi} + (U - \tilde{C}_{\vartheta i})^2} \tag{7}$$

The turbulence correlations are calculated following equations 8 to 13

$$\overline{C_{z,i}^{'2}} = \frac{1}{N} \sum_{n=1}^{N} (C_{z,i,n} - \tilde{C}_{z,i})^2 \tag{8}$$

$$\overline{C_{\vartheta,i}^{'2}} = \frac{1}{N} \sum_{n=1}^{N} (C_{\vartheta,i,n} - \tilde{C}_{\vartheta,i})^2 \tag{9}$$

$$\overline{C_{r,i}^{'2}} = \frac{1}{N} \sum_{n=1}^{N} (C_{r,i,n} - \tilde{C}_{r,i})^2 \tag{10}$$

$$\overline{C'_z C'^2_{\vartheta,i}} = \frac{1}{N}\sum_{n=1}^{N}(C_{z,i,n} - \breve{C}'_{z,i})(C_{\vartheta,i,n} - \breve{C}_{\vartheta,i})^2 \tag{11}$$

$$\overline{C'_z C'_{r,i}} = \frac{1}{N}\sum_{n=1}^{N}(C_{z,i,n} - \breve{C}_{z,i})(C_{r,i,n} - \breve{C}_{r,i})^2 \tag{12}$$

$$\overline{C'_\vartheta C'_z} = \frac{1}{N}\sum_{n=1}^{N}(C_{\vartheta,i,n} - \breve{C}_{\vartheta,i})(C_{r,i,n} - C_{r,i})^2 \tag{13}$$

The distribution of the three components of turbulence intensity in absolute flow

$$T_{z,i} = \frac{\sqrt{\overline{C'^2_{z,i}}}}{\breve{C}_i} \tag{14}$$

$$T_{\vartheta,i} = \frac{\sqrt{\overline{C'^2_{\vartheta,i}}}}{\breve{C}_i} \tag{15}$$

$$T_{r,i} = \frac{\sqrt{\overline{C'^2_{r,i}}}}{\breve{C}_i} \tag{16}$$

4. RESULTS OF SAMPLING AND DISCUSSION

4.1. Structure of Flow Downstream of the Impeller

The presented method was applied at first to measurements of a flow field on the middle radius 50 mm downstream of an axial flow rotating blade with the use of the straight and 90° versions of the triple splite fiber probes. A sequence of 100 real time samples of velocities were recorded over roughly 2 blade passing periods and averaged over 1000 revolutions.

Fig. 4 show the typical results of the ensemble–averaged mean axial $\breve{C}_z$, tangential $\breve{C}_\vartheta$ and radial $\breve{C}_r$ components of absolute velocity. The axial velocity shows a defect in velocity as each wake passes the probe, while the tangential velocity shows a peak, in phase with the axial velocity defect. It should be emphasised here that the most interesting information about the impeller flow is obtained from the analysis of the outlet relative velocity $\breve{W}$ and angle

β distribution (fig. 5). The region of a sudden decrease in the relative velocity indicates the blade wake of which the left side corresponds to the pressure side and other to the suction side. This makes it possible to find the values of profile boundary layer thickness. Also, taking into consideration the distribution of angle β, we can compare them with design blades angle and improve the aerodynamic calculation method.

Next, typical experimental results for turbulent characteristics are shown. Figure 6 show the distribution of six Reynolds stresses. In the calculation of

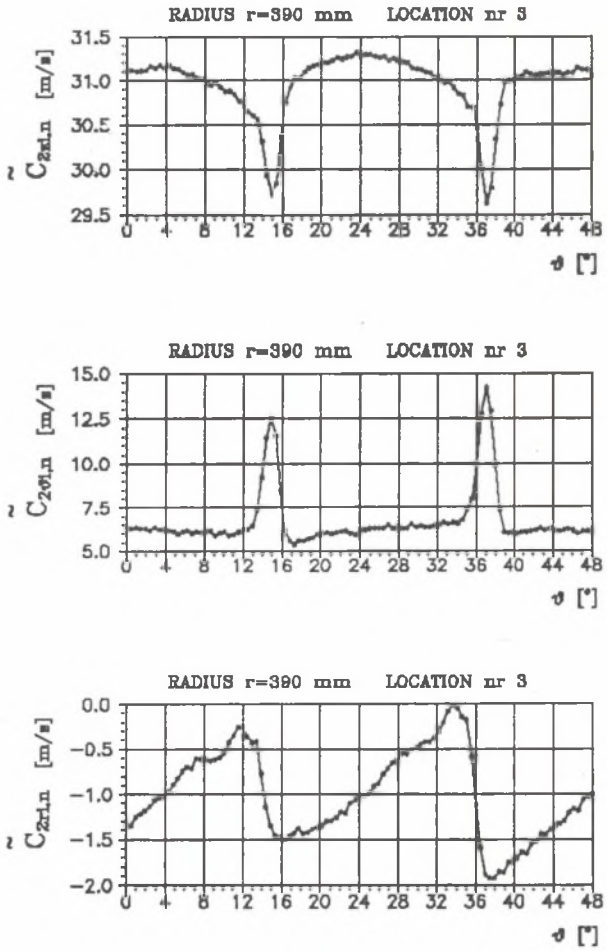

Fig. 4. Ensemble averaged components of absolute velocity at the exit of the impeller row

Rys. 4. Uśrednione grupowo składowe prędkości bezwzględnej

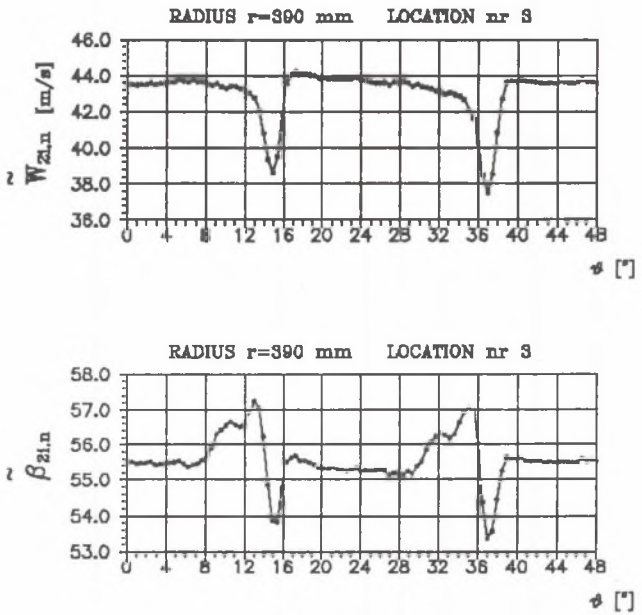

Fig. 5. Rotor blade wakes in the relative flow

Rys. 5. Ślad pozałopatkowy w przepływie względnym

the Reynolds stresses three components of the fluctuating velocity are taken as $C_z^{'}$ in the axial direction $C_\vartheta^{'}$ perpendicular to that velocity and $C_r^{'}$ in the radial direction. The distributions of the stresses are consistent with the velocity gradiens in terms of the turbulent shear flow theory.

The turbulence correlation plots at the position 3 (fig. 3) show clearly isotropic turbulence outside of the wake, and anisotropic turbulence in the wake region.

The distribution of the three components of turbulence intensity in absolute flow defined by equations 14, 15 and 16 are plotted in fig. 7. The turbulence intensities increase rapidly close to the impeller wake and attain the peak near the wake center line. The high turbulence intensities in this region indicate that the area of mixing the pressure and suctions side profile boundary layers is a highly active center of turbulence products. This can also be seen by a dramatic increase in turbulence correlation in fig. 6.

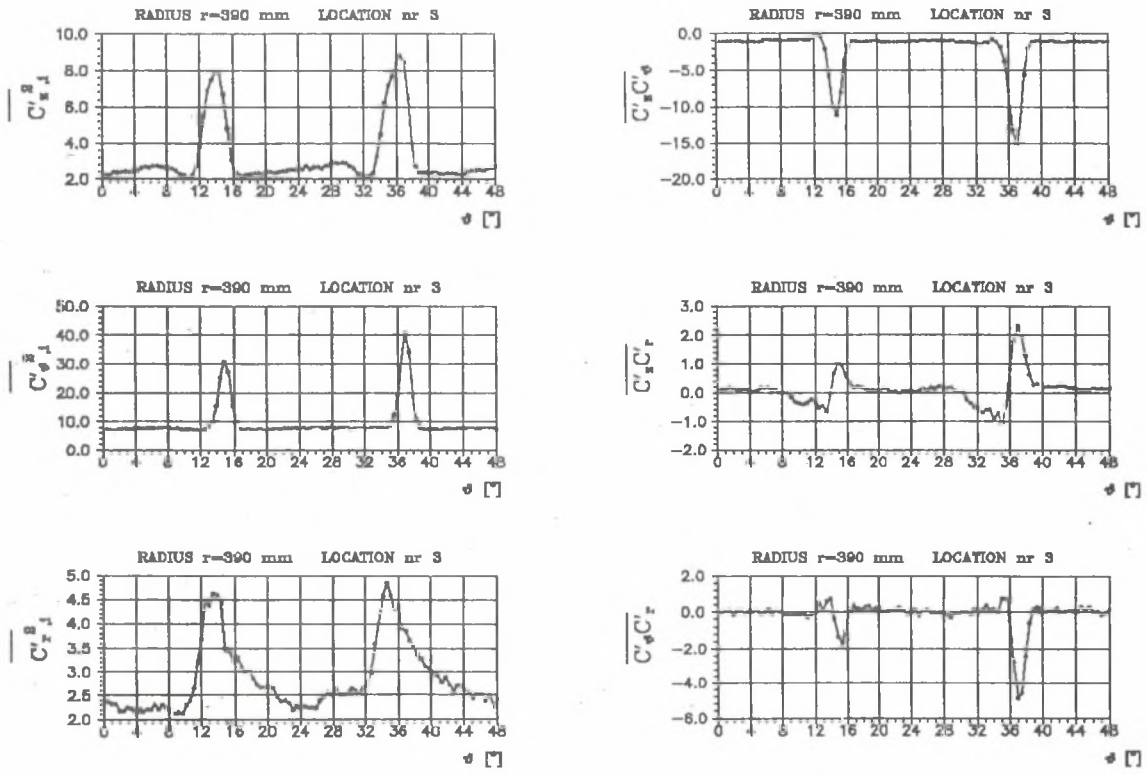

Fig. 6. Reynolds stresses distributions at the exit of the impeller row

Rys. 6. Rozkłady naprężeń Reynoldowskich w przekroju wylotowym koła wirnikowego

4.2. Decay characteristics of velocity and turbulence

In order to get basic understanding of the wake and turbulence intensities decay dependent on axial distance downstream of the impeller, the unsteady flow was determined at chosen axial location, preliminary on the middle radius only. Far downstream of the rotor the relative (fig. 8) and absolute (fig. 9) defect of the rotor wake decreasis significantly. It indicates that the axial distance of the rotor stator blade row was chosen properly. In a second step the wake decay was determined also along the centerline of the stator

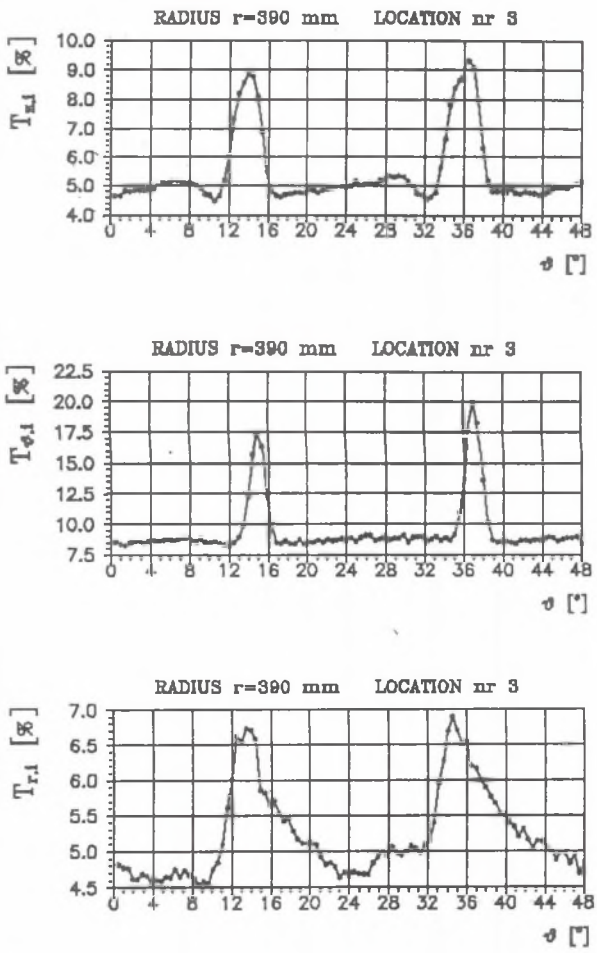

Fig. 7. Distributions of the turbulence intensities at the exit of the impeller row

Rys. 7. Rozkłady intensywności turbulencji w przekroju wylotowym koła wirnikowego

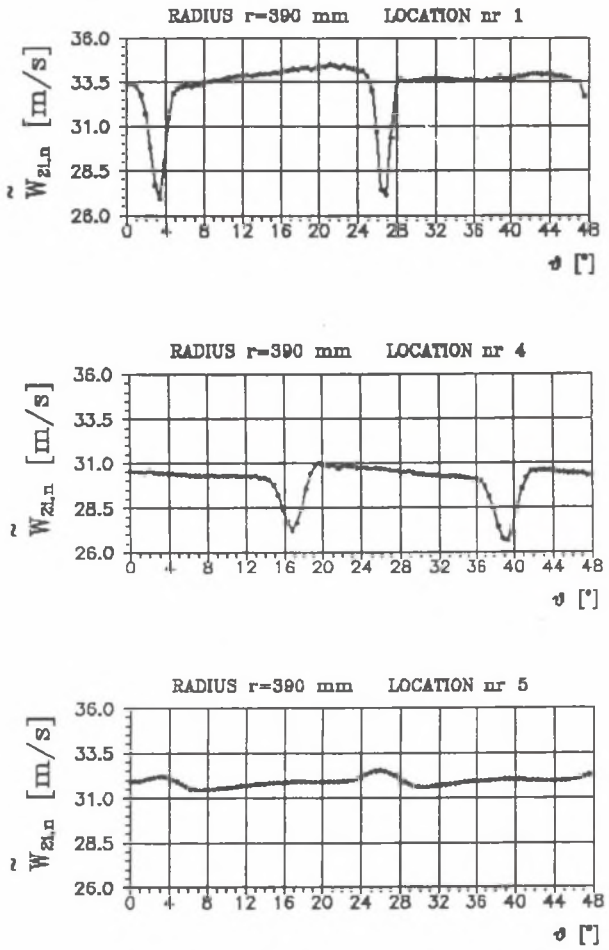

Fig. 8. Wake decay in relative flow

Rys. 8. Zanikanie śladu pozałopatkowego w przepływie względnym

blades in absolute frame of references. It was found that the wakes have been further smoothed continuosly by the presence of the stator. The absolute velocity wake depth (fig. 9) decreasis from 4 m/s at location 1 just downstream of the trailing edge of the impeller blade to 0.4 m/s at location 17.

Decrease of the rotor blade wake causes lower velocity gradients normal to the wake. Therefore the components of the turbulence production in the wake (figs. 10 and 11) decreases in location downstream of the rotor due to the

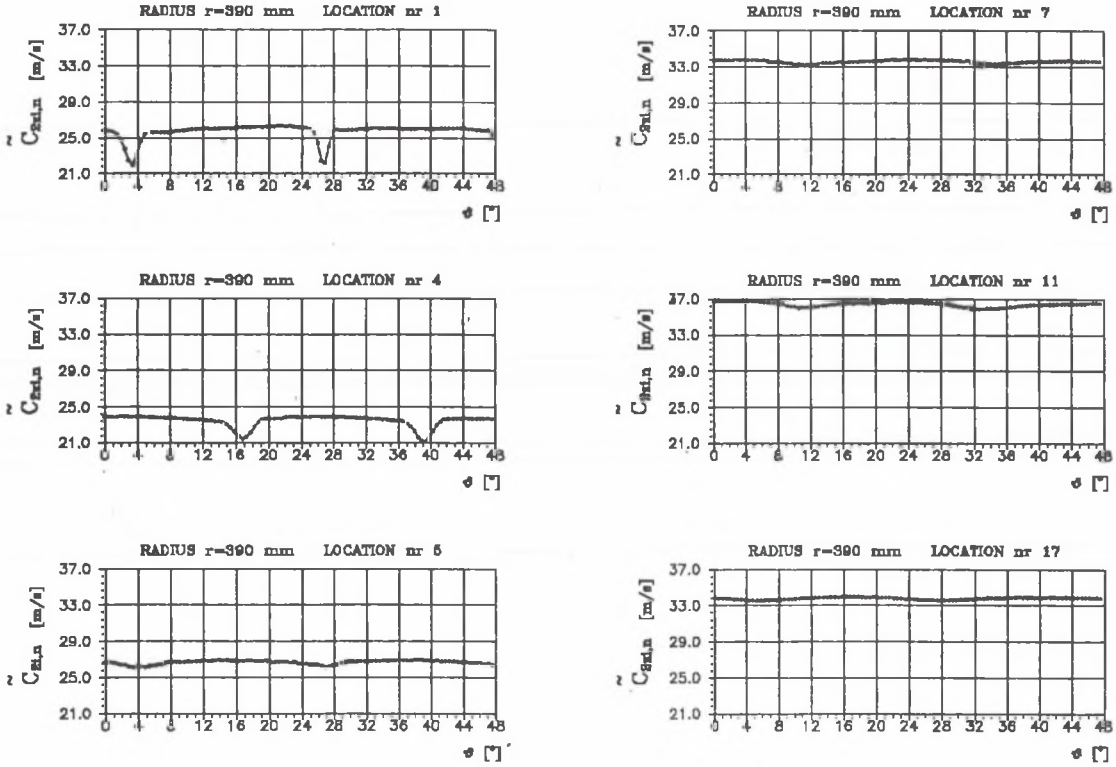

Fig. 9. Wake decay in absolute flow

Rys. 9. Zanikanie śladu pozałopatkowego w przepływie bezwzględnym

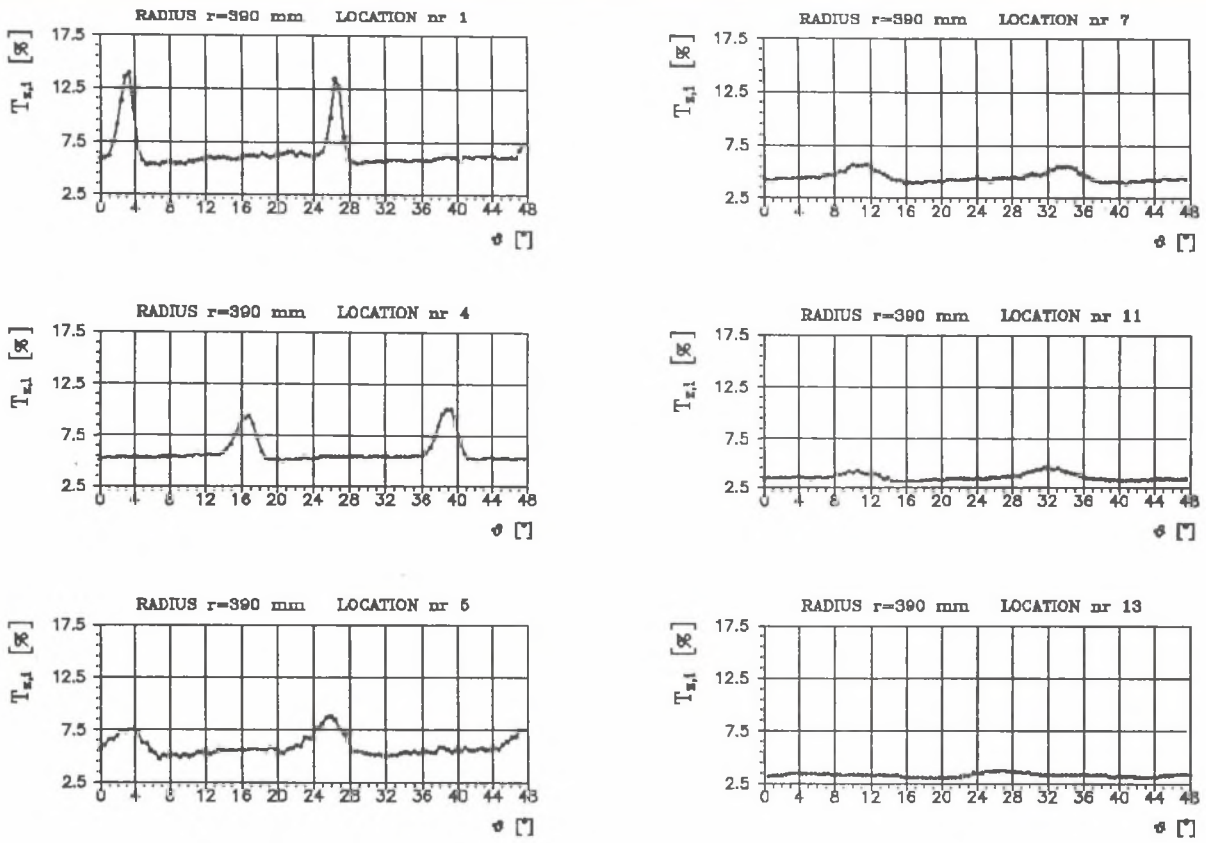

Fig. 10. Decay of axial component of turbulence intensity

Rys. 10. Zanikanie składowej osiowej intensywności turbulencji

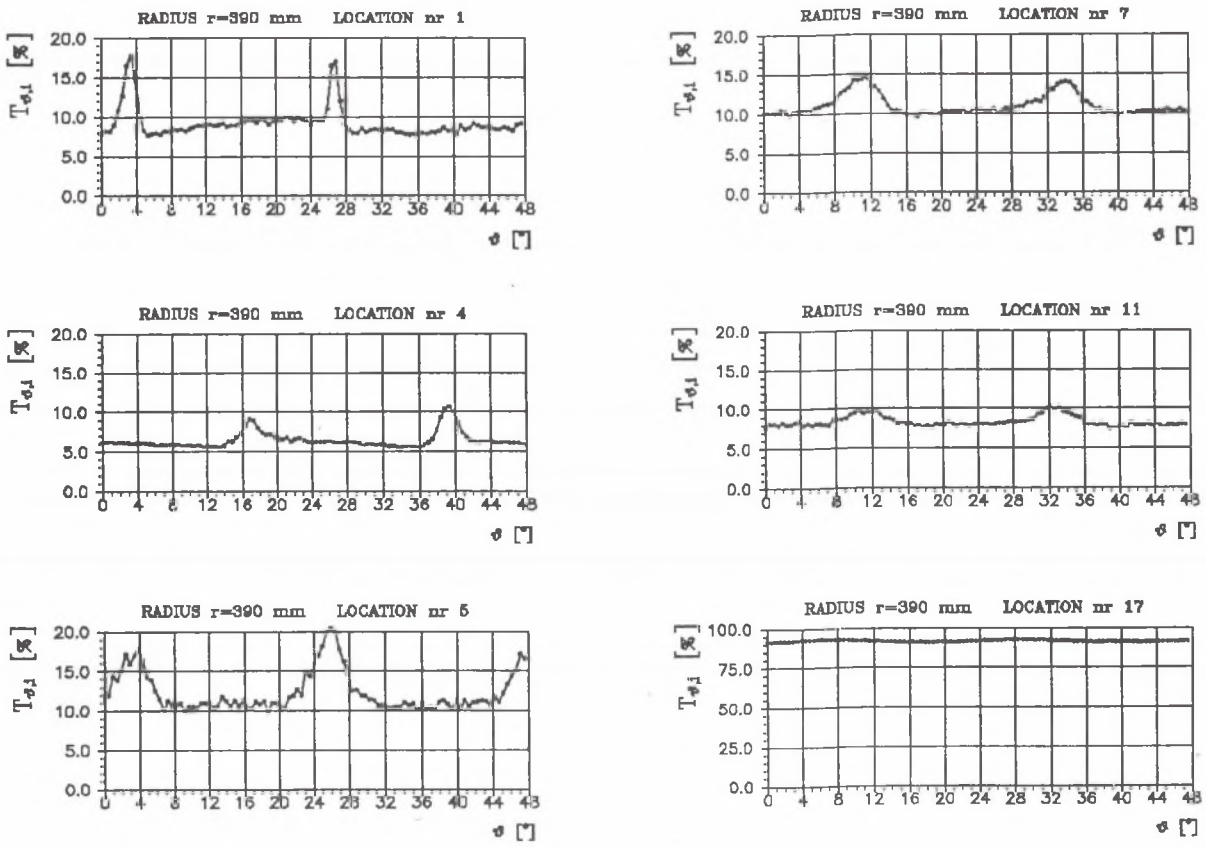

Fig. 11. Decay of tangential component of turbulence intensity

Rys. 11. Zanikanie składowej obwodowej intensywności turbulencji

mixing effects. There are significant diffrences in the decay characteristics of the axial and tangential components of wake of a velocity, turbulence intensities and turbulence correlation in blade row spacing. Tangential components of turbulent intensities and turbulent correlation strongly increasis on a plane just upstream of the inlet edges of the stator blades as a results of its backward reaction (fig. 11). It causes that the level of tangential turbulence intensity and turbulence correlation inside stator blade passage is considerably higher than the axial ones.

4.3. The spanwise characteristics of the unsteady flow

In order to get the spanwise characteristics of the unsteady flow the 39 radial measurements were carried out just downstream of the blade impeller. Figs. 12, 13, 14, 15 and 16 show the comparison of relative and absolute components of rotor blade wake, turbulence intensities and turbulence correlation at the three radius: at the hub, on the middle radius of the impeller and at the outer wall. Near the tip of the rotor, the flow pattern is very complex. Leakage flow, the mixing of pressure and suction side profile

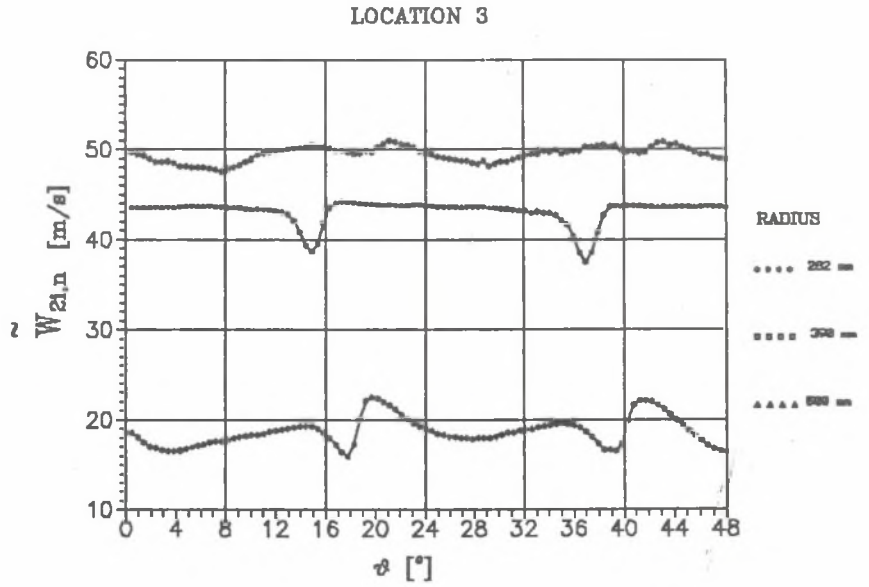

Fig. 12. Comparison of the circumferencial distribution of the relative velocities at the three diffrent radius

Rys. 12. Porównanie rozkładów obwodowych prędkości względnych na trzech promieniach

boundary layers, horseshoe vortex and irregular shed van Karman vortices are superimposed. So that phenomena strongly influence the exit velocity distribution in the relative frame and caused significatly higher turbulence in that region.

4.4. Secondary flow

In the next figure 17 the secondary flows relative and absolute to the blade are illustrated by the distribution in vector form of the velocity components which represent departures from the design potential flow field. The secondary velocity is the resultant of W_r, the radial component, and W_ϑ the circumferential component of velocity. In the wake area, the inbalance between centrifugal and pressure forces causes inward directed on the middle radius and upward directed at hub and at the outer wall radial component of velocity.

The turbulence structure in the secondary flow region near the corner stall separation is not isotropic.

5. CONCLUSIONS

The work presented here has a character of preliminary study, the more so, that the measurements have been taken for only one, maximum value of velocity coefficient $\varphi = C_m/U_2$. The results of the experiments shows that triple split fiber probes straight and 90° measurements combined with ensemble everage technique are the very useful method for the analysis of rotor flow in turbomachinery. Tip clearance vortex, secondary flow near the hub, and radial flow in the wake, turbulent intensity and Reynolds stresses and so on the decay of the rotor wakes can be obtained by this method which provides knowledge on the turbulent characteristics of the wake in connection with the wake behavior. From the experimental result reported in this paper the following coclusions are drawn:

1. The turbulence structure of the wake in the location 3 is not isotropic. The axial and circumferential turbulence intensities are smaller then the radial ones. The maximum turbulence intensities in the rotor wake reach values of about 12,5 percent when radial ones 24,5 percent.
2. The highest fluctuations of the velocity, the flow angle and the turbulence intensity are detected in the hub and tip region. These results suggest that the radial distribution of the flow properties should be included into the design process.
3. Far downstream of the rotor wake decreasis specificantly so it doesn't influenced the flow in stator passages. That method get us possible to find the proper axial distance between rotor and stator blade rows.

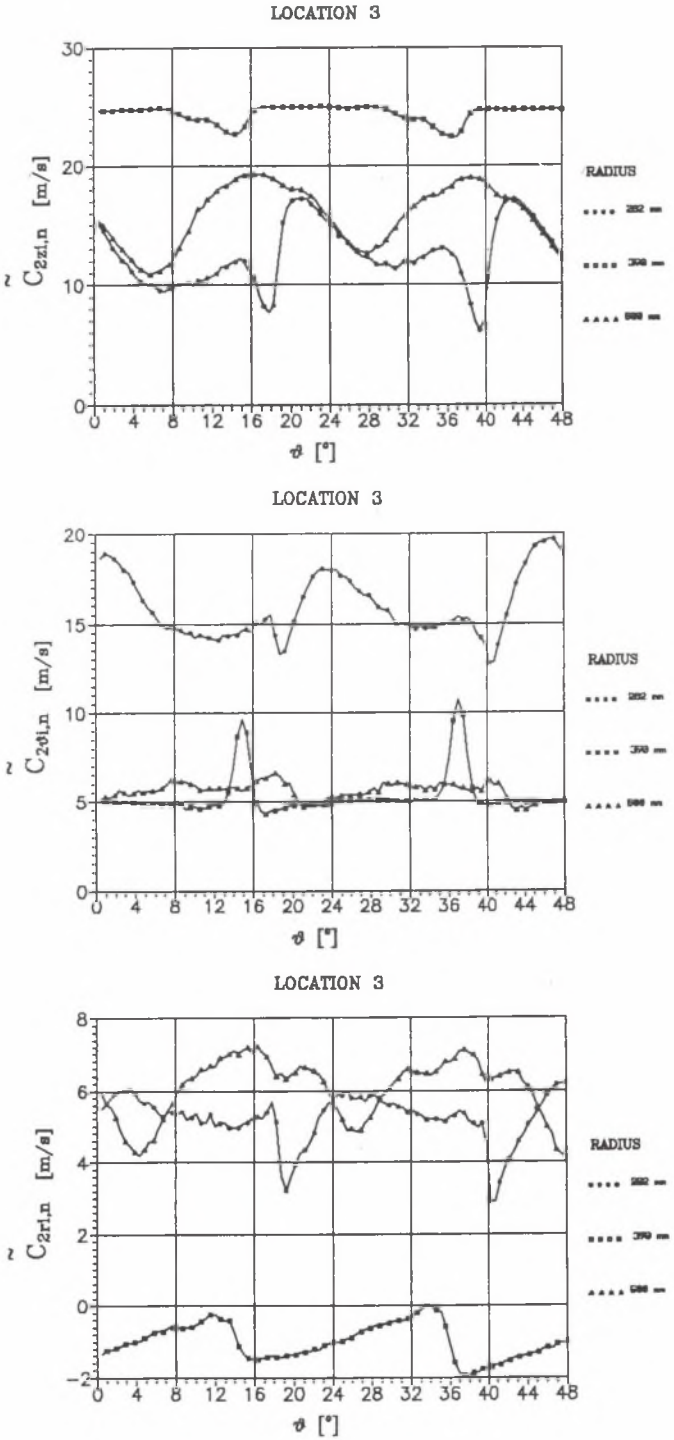

Fig. 13. Comparison of the circumferencial distribution of the absolute components of volocities at the three diffrent radius

Rys. 13. Porównanie rozkładów składowych prędkości bezwzględnej w kierunku obwodowym na trzech promieniach

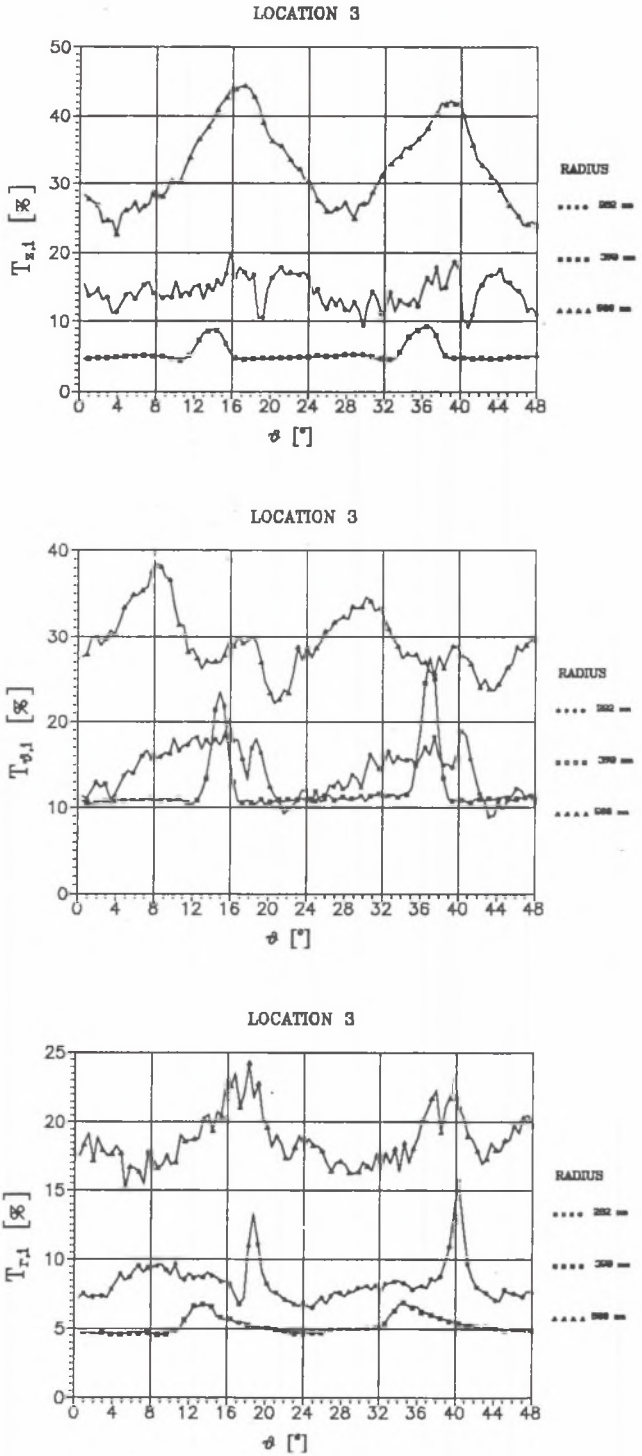

Fig. 14. Comparison of the turbulence intensities at the three radius downstream of the impeller

Rys. 14. Porównanie intensywności turbulencji na trzech promieniach w przekroju wylotowym koła wirnikowego

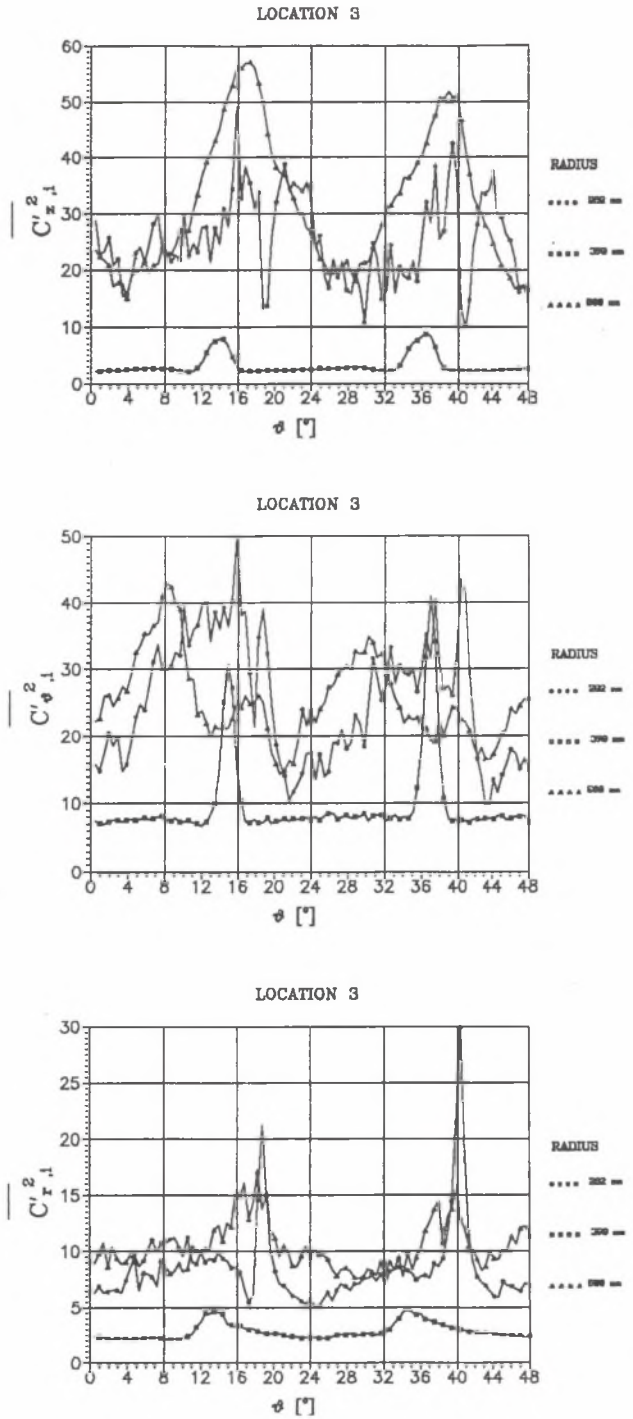

Fig. 15. Comparison of the Reynolds stresses at the three radius downstream of the impeller

Rys. 15. Porównanie trzech składowych naprężeń Reynoldowskich w przekroju wylotowym koła wirnikowego

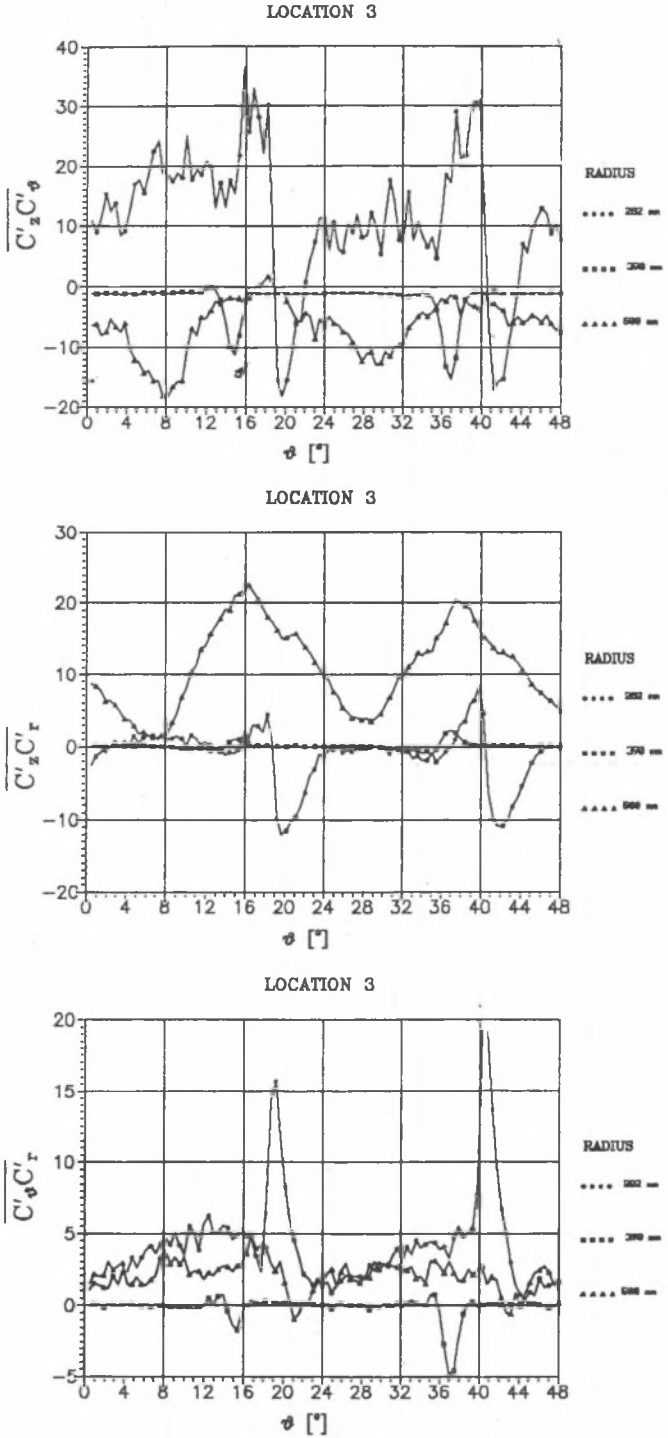

Rys. 16. Comparison of the turbulence correlation at the three radius downstream of the impeller

Rys. 16. Porównanie trzech składowych funkcji korelacyjnych turbulencji na trzech promieniach w przekroju wylotowym koła wirnikowego

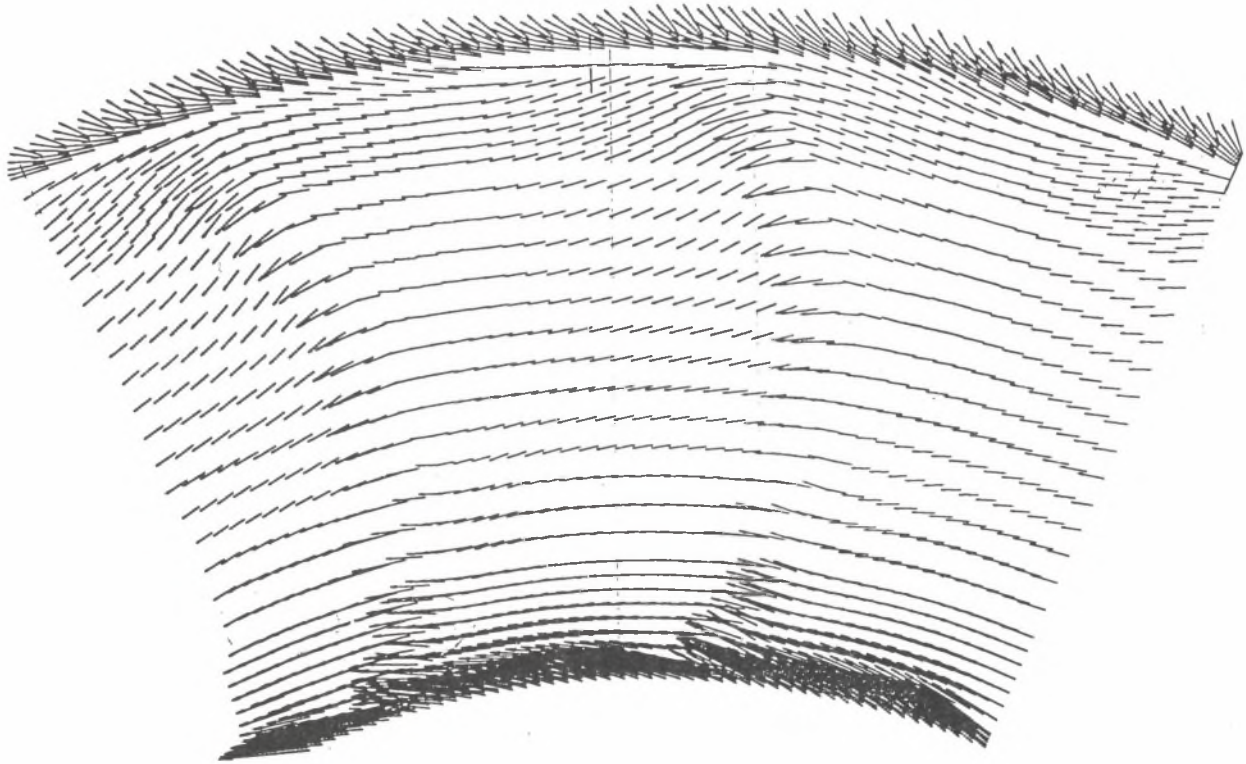

Rys. 17. Secondary Flow Field in the absolute (a) and relative (b) System Downstream of the Rotor

Rys. 17. Pole przepływów wtórnych w bezwzględnym i względnym układzie w przekroju wylotowym koła wirnikowego

Further experimental and theoretical work is necessary on these topics. For high simulation levels of the compressor flow many authors [7], [8], [9] feel that only modeling of the fully three dimensional unsteady and viscous flow will produce sufficiently accurate predictions.

REFERENCES

[1] Witkowski A., Chmielniak T., Strozik M., Mirski M.: Stand for investigations of threedimensional turbulent flow in axial compressing stage. Archiwum Budowy Maszyn, nr 3/4, 1994 (w druku).
[2] Witkowski A., Chmielniak T., Strozik M., Mirski M.: Metoda pomiaru turbulencji i zjawisk nieustalonych w stopniu wentylatora osiowego. Zeszyty Naukowe Pol. Śl., seria Energetyka, z. 118, Gliwice 1993.
[3] Jörgensen F.E.: Characteristics and Calibration of a Triple–Split Probe for Reversing Flows. DISA Information No 27, 1982.
[4] Witkowski A., Chmielniak T., Strozik M., Mirski M.: Turbulence Measurements in an Axial Flow Low Pressure Compressor Stage with the Use of Triple Split Fiber Probes. VDI Berichte 1186. First European Conference, Erlangen, March 1995.
[5] Bendat I.S., and Piersol A.G.: Random Data Analysis and Measurement Procedures. Wiley, New York 1986, pp. 425–483.
[6] Lakshminarayana B., and Poncet A.: A Method of Measuring Threedimensional of Rotating Wakes Behind Turbomachinery Rotors. ASME, Journal of Fluids Engineering, vol. 96, pp. 871–916, 1974.
[7] Gallus A.E., Poensgen C., Zeschky J.: A Comparison between the Unsteady Flow Fields in an Axial Flow Compressor and an Axial Flow Turbine. European Propulsion Forum, November 1992, Paris.
[8] Schultz A.D., Gallus A.E.: Experimental Investigation of the Three–Dimensional Flow in an Annulur Compressor Cascade Journal of Turbomachinery, vol. 110, 1981.
[9] Moore J., Moore J.G., Heckel S.P., Bellesteros R.: Reynolds Stresses and Dissipations Mechanisms in a Turbine Tip Leakage Vortex. ASME 94 GT–141, 1994.

Streszczenie

Większość współczesnych metod obliczeń przepływowych i projektowania stopni maszyn wirnikowych opracowano na podstawie informacji uzyskanych z analizy stacjonarnego przepływu. Przepływ niestacjonarny, wynikający z występowania przepływów wtórnych oraz wzajemnego oddziaływania wieńców łopatkowych, posiada istotny wpływ na pole przepływu, warstwy przy-

ścienne, intensywność turbulencji, oderwania strug, drgania oraz hałaśliwość pracy. Współczesne tendencje występujące w projektowaniu maszyn przepływowych zmierzające do zmniejszenia przestrzeni międzywieńcowych w stopniach, zmniejszenia stosunku średnic oraz zwiększenia obciążenia aerodynamicznego łopatek stwarzają dodatkowe warunki potęgujące zjawiska niestacjonarne w przepływie. Wszystko to sprawia, że niezbędne staje się opracowanie metod obliczeniowych uwzględniających zjawiska niestacjonarne w przepływie oraz modelowanie turbulencji. Wprawdzie metody analizy przepływu osiągnęły znaczny postęp w ostatnich latach, modelowanie turbulencji pozostaje nadal zagadnieniem bardzo trudnym głównie z uwagi na brak danych eksperymentalnych. Stąd szczegółowe rozpoznanie na drodze eksperymentalnej przepływów wtórnych, śladów pozałopatkowych, struktury turbulencji, rozprzestrzeniania się tych zjawisk w przestrzeni pomiędzy wieńcem łopatkowym koła wirnikowego i kierownicy tylnej, jak również w kanałach międzyłopatkowych kierownicy tylnej, w wybranych punktach charakterystyki aerodynamicznej, jest niezbędne zarówno dla weryfikacji numerycznych algorytmów przepływów przestrzennych, jak i procedur projektowych maszyn przepływowych. Wychodząc z tych przesłanek opracowano w Instytucie Maszyn i Urządzeń Energetycznych system periodycznego, wielopróbkowego sondowania nieustalonego, przestrzennego pola prędkości w osiowym stopniu sprężającym, w układzie bezwzględnym. System umożliwia zbieranie do 3000 sekwencji pomiarowych w czasie jednej minuty, składających się ze 100 próbek prędkości równomiernie rozmieszczonych wzdłuż obwodu obejmującego swym zasięgiem dowolną, wybraną liczbę łopatek koła wirnikowego. Przeprowadzone w jednym punkcie charakterystyki aerodynamicznej, wstępne próbkowania pola prędkości przy wykorzystaniu sondy cylindrycznej prostej i kątowej, z trójdzielną warstwą w skojarzeniu z metodą uśredniania grupowego, wskazują na możliwość stosunkowo szybkiego i dokładnego wyznaczania wielkości charakteryzujących przepływ turbulentny w wybranych przekrojach przestrzeni międzywieńcowych stopnia oraz w kanałach międzyłopatkowych kierownicy tylnej. Potwierdzają to zamieszczone w referacie wyniki zawierające badania zanikania śladu pozałopatkowego koła wirnikowego struktury turbulencji oraz próbę przedstawienia obrazu przepływów wtórnych za kołem wirnikowym.